Chapter 1 Introduction

Due to their high specific strength and stiffness properties, fiber-reinforced thin-walled composite cylinders have numerous applications in the aerospace industry as structural elements. Although circular cylinders are most commonly used and studied, future transport fuselages could have noncircular cross sections, in particular, oval or elliptical cross sections. A noncircular cross section could be beneficial for blended wing-fuselage structural concepts, improved aerodynamics, and increased payload capacity. A number of issues associated with noncircular cross sections must be addressed. These issues include the effect of noncircular geometry, geometric nonlinearities, boundary conditions, loading, and material orthotropy. This study is concerned with internal pressurization, which is an important loading for fuselage structures, and cylinders with elliptical cross sections. There are a number of fundamental issues with this particular loading. For example, a circular cylinder subjected to internal pressure expands outward, whereas, an elliptical cylinder becomes more circular in shape, as shown in fig. 1-1. For an elliptical cylinder, deflections are actually inward at certain circumferential locations. Additionally, with internal pressure there is a net axial force on each end of the cylinder. Assumptions regarding how this force is reacted by the cylinder have an impact on the assumed conditions at the boundary. These concerns are addressed in the present study by using a semi-analytical approach to obtain numerical results. These results are then used to illustrate the differences between a circular and elliptical cross section cylinders, and geometrically linear and nonlinear effects. Also, the influence of orthotropy is discussed, specifically, quasi-isotropic, axially-stiff, and circumferentially-stiff

graphite-epoxy laminates are considered. Failure is addressed. The semi-analytical approach, developed in a previous study [1], utilizes the Kantorovich and finite-difference techniques to solve the governing equations. A description of the details of the specific problem and of the semi-analytical approach is described in the next two sections. The following section outlines the contents of the remainder of this document.

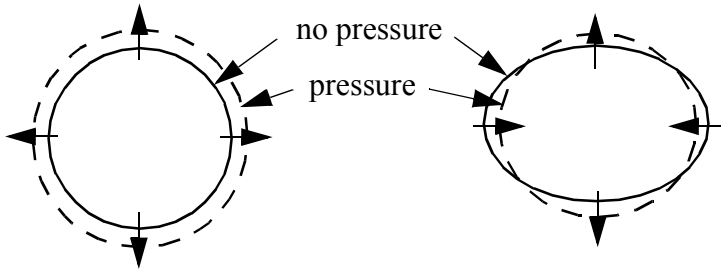

Figure 1-1. Effect of internal pressure on cross-sectional deformation of an ellipse.

1.1 Problem Description

The problem considered consists of a cylinder described in fig. 1-2, with a, b, and L denoting, respectively, the semi-major diameter, semi-minor diameter, and axial length of the cylinder reference surface. The degree of ellipticity, e, is defined here as the ratio of the semi-minor and major diameters, b/a. Alternatively, b/a can be thought of as the cross-sections aspect ratio. The cylinders considered here are symmetrically laminated and have an ellipticity of 0.7 and 1.0, the latter corresponding to a circular cylinder. The wall thickness of the cylinder is denoted by H and the internal pressure by p_o. The upper part of the cross-section is referred to as the crown, the lower part as the keel, and the sides are referred to as the sides.

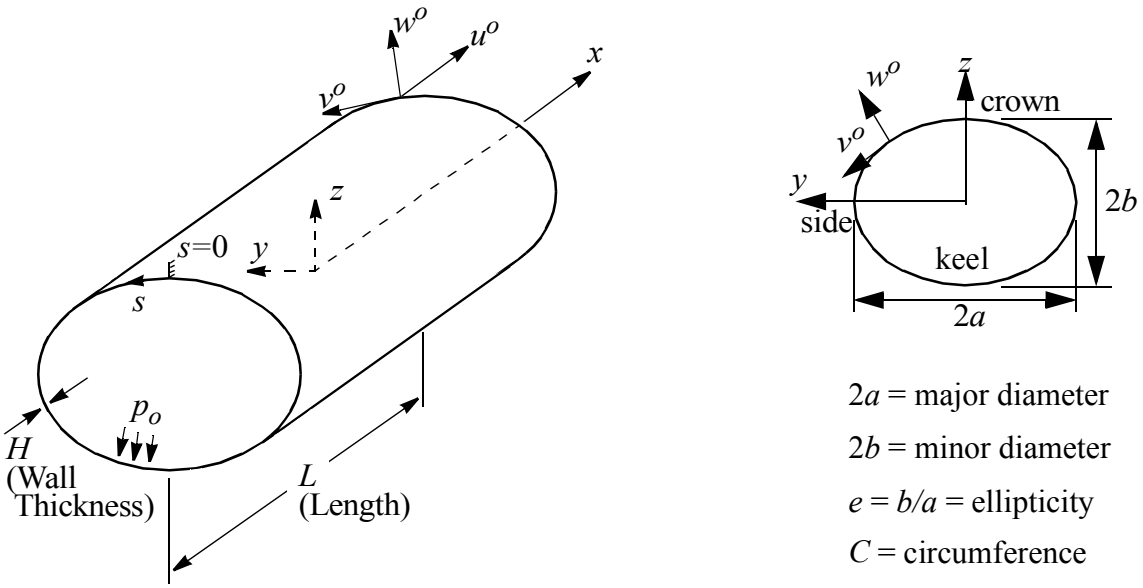

Figure 1-2. Problem description, nomenclature, and geometry of an elliptical cylinder.

The cross sectional shape of the cylinder at the reference surface, or midwall location, is an ellipse lying in the global y-z plane described by

$$\frac{y^2}{a^2} + \frac{z^2}{b^2} = 1. \tag{1.1}$$

The maximum and minimum radii of curvature are

$$R_{MAX} = \frac{a^2}{b} \qquad \text{and} \qquad R_{MIN} = \frac{b^2}{a}, \tag{1.2}$$

which occur at the ends of the semi-minor and -major axes, respectively. Locations on the reference surface are identified by coordinates (x,s), where x is the axial coordinate, measured from the midspan location, and s is the circumferential arc-length coordinate, measured counterclockwise from the top, or crown, of the cylinder. The reference surface displacement in the axial and circumferential directions are denoted as $u^o(x,s)$ and $v^o(x,s)$, respectively, while the normal displace-

ment is denoted by $w^o(x,s)$. Herein, only thin cylinders are discussed, and the orientation of the layers is defined relative to the $+x$ axis in the laminate nomenclature. Here it will be assumed the cylinder ends are clamped to a rigid end plate or bulkhead which can move axially. Accordingly, clamped-clamped boundary conditions are applied to each end of the cylinder, with the exception of allowing the end at $x = +L/2$ end to expand uniformly in the axial direction with displacement Δ. The end at $x = -L/2$ cannot move axially in order to restrict axial rigid body translation. Formally, the boundary conditions at the ends of the cylinder ($x = \pm L/2$) are as follows:

$$\begin{aligned} &\text{i)}\ u^o = 0\ @\ x = -\frac{L}{2},\ u^o = \Delta\ @\ x = +\frac{L}{2} \\ &\text{ii)}\ v^o = 0 \\ &\text{iii)}\ w^o = 0 \\ &\text{iv)}\ \frac{\partial w^o}{\partial x} = 0. \end{aligned} \tag{1.3}$$

The end displacement Δ is determined by enforcing axial equilibrium of the end enclosure at $x = +L/2$, namely,

$$\int_0^C N_x ds = p_o \pi ab, \tag{1.4}$$

where N_x is the axial force resultant within the cylinder (to be defined shortly), C is the circumference of the cylinder reference surface, and the cross-sectional area of the ellipse is πab. Physically, eq. 1.4 states that the net axial force due to the internal pressure times the cross-sectional area of the end enclosure must be balanced by the net axial force due to the axial force resultant.

1.2 Solution Approach

The semi-analytical solution procedure begins with the expression for the total potential energy of the cylinder. The total potential energy is given by

$$\pi = \frac{1}{2}\int\int\int [\sigma_x \varepsilon_x + \sigma_s \varepsilon_s + \tau_{xs}\gamma_{xs}]\, dx\, ds\, d\zeta - \int\int p_o w^o\, dx\, ds, \tag{1.5}$$

where ζ is the local through-thickness coordinate within the cylinder wall. The coordinate ζ ranges from $-H/2 \le \zeta \le +H/2$ and is zero at the reference surface. Of course the axial coordinate has the limits from $-L/2 \le x \le +L/2$, and the circumferential coordinate has the limits from $0 \le s \le C$. As evidenced by the integrand in eq. 1.5, the plane-stress assumption is being used. The strains in the energy expression are given by

$$\begin{aligned} \varepsilon_x &= \varepsilon_x^o + \zeta \kappa_x^o \\ \varepsilon_s &= \varepsilon_s^o + \zeta \kappa_s^o \\ \gamma_{xs} &= \gamma_{xs}^o + \zeta \kappa_{xs}^o, \end{aligned} \tag{1.6}$$

where the reference surface strains and curvatures are related to the reference surface displacements by

$$\varepsilon_x^o = \frac{\partial u^o}{\partial x} + \underline{\frac{1}{2}\left(\frac{\partial w^o}{\partial x}\right)^2} \tag{a}$$

$$\varepsilon_s^o = \frac{\partial v^o}{\partial s} + \frac{w^o}{R(s)} + \underline{\frac{1}{2}\left(\frac{\partial w^o}{\partial s}\right)^2} \tag{b}$$

$$\gamma_{xs}^o = \frac{\partial u^o}{\partial s} + \frac{\partial v^o}{\partial x} + \underline{\left(\frac{\partial w^o}{\partial x}\right)\left(\frac{\partial w^o}{\partial s}\right)} \tag{c}$$

$$\kappa_x^o = -\frac{\partial^2 w^o}{\partial x^2} \tag{d}$$

$$\kappa_s^o = -\frac{\partial^2 w^o}{\partial s^2} \tag{e}$$

$$\kappa_{xs}^o = -2\frac{\partial^2 w^o}{\partial x \partial s}. \tag{f}$$

(1.7)

Note that the radius of curvature being a function of s in $\varepsilon^o{}_s$ is what makes this problem different than that of a circular cylinder. The underlined terms in eq. 1.7a-c denote the geometric nonlinear-

ities. These are the von Karman approximations to the fully nonlinear strain-displacement relations. Substituting eq. 1.6 into eq. 1.5 and integrating the energy expression through the thickness of the cylinder wall results in

$$\pi = \frac{1}{2}\int\int [N_x\varepsilon_x^o + N_s\varepsilon_s^o + N_{xs}\gamma_{xs}^o + M_x\kappa_x^o + M_s\kappa_s^o + M_{xs}\kappa_{xs}^o - p_o w^o]\,dx\,ds \quad \text{(a)}$$
$$= \int\int U(x, s)\,dx\,ds, \quad \text{(b)} \tag{1.8}$$

where eq. 1.8b serves as the reminder that the integrand is strictly a function of x and s. The force and moment resultants in eq. 1.8 are defined by

$$\begin{aligned}
N_x &= \int \sigma_x d\zeta = A_{11}\varepsilon_x^o + A_{12}\varepsilon_s^o \\
N_s &= \int \sigma_s d\zeta = A_{12}\varepsilon_x^o + A_{22}\varepsilon_s^o \\
N_{xs} &= \int \tau_{xs} d\zeta = A_{66}\gamma_{xs}^o \\
M_x &= \int \sigma_x \zeta d\zeta = D_{11}\kappa_x^o + D_{12}\kappa_s^o + D_{16}\kappa_{xs}^o \\
M_s &= \int \sigma_s \zeta d\zeta = D_{12}\kappa_x^o + D_{22}\kappa_s^o + D_{26}\kappa_{xs}^o \\
M_{xs} &= \int \tau_{xs} \zeta d\zeta = D_{16}\kappa_x^o + D_{26}\kappa_s^o + D_{66}\kappa_{xs}^o.
\end{aligned} \tag{1.9}$$

where, as seen from the form of eq. 1.9, only symmetric and balanced laminates [2] are being considered.

With the radius of curvature varying circumferentially, a closed-form solution to the problem is not easily found. Accordingly, an approximate solution is sought. To begin the approximate solution, the circumferential variation of the radius of curvature is expanded, in a method suggested by Marguerre [3], in a cosine series such that,

$$\frac{1}{R(s)} \cong \sum_{i=0}^{I} a_{4i}\cos(4i\pi s/C), \tag{1.10}$$

where the coefficients a_{4i} are constants which depend on the specific cross-sectional geometry (semi-diameters a and b) and I is the number of terms needed to properly represent the variation of the inverse radius of curvature. The dependence of the reference surface displacements on the circumferential coordinate is approximated using the Kantorovich method by a harmonic series in a form inspired by the inverse radius of curvature, namely,

$$\begin{aligned} u^o(x,s) &= u_o^o(x) + \sum_{n=1}^{N} u_n^o(x)\cos(4n\pi s/C) + \sum_{m=1}^{M} u_{N+m}^o(x)\sin(4m\pi s/C) \\ v^o(x,s) &= v_o^o(x) + \sum_{m=1}^{M} v_m^o(x)\cos(4m\pi s/C) + \sum_{n=1}^{N} v_{M+n}^o(x)\sin(4n\pi s/C) \\ w^o(x,s) &= w_o^o(x) + \sum_{n=1}^{N} w_n^o(x)\cos(4n\pi s/C) + \sum_{m=1}^{M} w_{N+m}^o(x)\sin(4m\pi s/C). \end{aligned} \tag{1.11}$$

Both sines and cosines are used to represent all three displacement components, where M and N determine the number of terms of each. For an isotropic cylinder, sine terms would not be necessary for $u^o(x,s)$ and $w^o(x,s)$, while cosine terms would not be necessary for $v^o(x,s)$. The presence of the bending stiffness terms D_{16} and D_{26} makes inclusion of these terms necessary.

With eq. 1.10 and eq. 1.11, the displacements and the radius of curvature have been explicitly expressed in terms of the circumferential coordinate, s. Substituting the displacements of eq. 1.11 into the strains and curvatures of eq. 1.7, and the stress and moment resultants of eq. 1.9 into the energy expression of eq. 1.8, integration of the energy expression can be performed with respect to s. The integrand of the energy expression is then dependent on the coefficients in eq. 1.11, which are only a function of x. As a result, the energy expression can be written symbolically as

$$\pi = \int_{-\frac{L}{2}}^{+\frac{L}{2}} \left[\int_0^C U(x,s)ds \right] dx$$
$$= \int_{-\frac{L}{2}}^{+\frac{L}{2}} F(y_i(x), y'_i(x), y''_i(x))dx; \qquad i = 1, 3(N + M + 1) \tag{1.12}$$

In the above the $y_i\,(x)$ represent the functional coefficients in eq. 1.11 and ( )' represents differentiation with respect to the axial coordinate x. Although the integrand above is also a function of cylinder geometry, material properties, and the pressure, they are constants that are not involved in the variational process. Equating the first variation of the total potential energy to zero results in the Euler-Lagrange equations for the $y_i(x)$ and the associated variationally consistent boundary conditions at $x = \pm L/2$. In general terms, the Euler-Lagrange equations are

$$\frac{d^2}{dx^2}\left(\frac{\partial F}{\partial y_i''}\right) - \frac{d}{dx}\left(\frac{\partial F}{\partial y_i'}\right) + \frac{\partial F}{\partial y_i} = 0 \tag{1.13}$$

and the boundary conditions are

$$y_i' \text{ specified} \qquad \text{or} \qquad \frac{\partial F}{\partial y_i''} = 0$$
$$y_i \text{ specified} \qquad \text{or} \qquad \frac{d}{dx}\left(\frac{\partial F}{\partial y_i''}\right) - \frac{\partial F}{\partial y_i'} = 0. \tag{1.14}$$

The boundary conditions of eq. 1.3 translate into specifying values of $y_i(x)$ and $y_i'(x)$. Defining intermediate variables in order to reduce the system from a third-order to a first-order form, it is possible to obtain a set of coupled nonlinear first-order ordinary differential equations of the form

$$\bar{y}_i'(x) = f_i(\bar{y}_i'(x)); \qquad i,j = 1, 8(N + M + 1), \tag{1.15}$$

where

$$\bar{y}_i(x) = \{u_k^o, v_k^o, w_k^o, q_k, r_k, t_k, g_k, h_k\}; \qquad k = 1, 8(N + M + 1) \tag{1.16}$$

and

$$q_k = \frac{dw_k^o}{dx}, \quad r_k = \frac{dq_k}{dx}, \quad t_k = \frac{dr_k}{dx}, \quad g_k = \frac{du_k^o}{dx}, \quad h_k = \frac{dv_k^o}{dx}. \tag{1.17}$$

This process has been automated using the symbolic manipulation package *Mathematica*©[4]. The resulting differential equations in x are written into FORTRAN code using the FORTRANASSIGN package within *Mathematica*©. These equations are integrated by the finite-difference method using the IMSL subroutine DBVPFD [5] which is based on a variable-order, variable-step-size algorithm employing Newton's method. By rendering the governing Euler-Lagrange equations to first-order form, as in eq. 1.17, various derivatives of u^o, v^o, and w^o are directly available for computing reference surface strains and curvatures and force and moment resultants. More importantly, stresses as a function of x, s, and ζ can be computed.

1.3 Remainder of Document

In the following chapters, using numerical results, a thorough explanation will be given of the effects of cylinder geometry, specifically circular vs. elliptical cross sections, and geometric nonlinearities on cylinder responses. Also, the effects of orthotropy will be studied using quasi-isotropic, axially-stiff, and circumferentially-stiff graphite-epoxy laminates. Displacements, reference surface strains and curvatures, and force and moment resultants will be used to define cylinder responses. A comparison of these cylinder responses will be made with finite-element analysis to verify the numerical results. These discussions will take place in chapters 2, 3 and 4. In chapters 5 and 6, two failure theories, the Hashin failure theory and the maximum stress theory, will be used to assess the pressure capacity of elliptical composite cylinders. Interlaminar shear stresses are considered by integrating the geometrically linear equilibrium equations of elasticity in polar coordinates through the thickness at the cylinder wall. These interlaminar shear stresses

together with the inplane (intralaminar) stresses are used in the failure theories. Failure pressure levels, failure location, and failure modes are studied. Finally, conclusions of this work will be presented, and future directions discussed.